

Journal Pre-proof

Synthesis and characterization of alkenyl and alkyl substituted group 4 metallocene dichloride complexes: Applications in ethylene polymerization

Jesús Ceballos-Torres, Santiago Gómez-Ruiz, Mariano Fajardo, Ana B. Pinar, Sanjiv Prashar



PII: S0022-328X(19)30333-X

DOI: <https://doi.org/10.1016/j.jorganchem.2019.120890>

Reference: JOM 120890

To appear in: *Journal of Organometallic Chemistry*

Received Date: 15 May 2019

Revised Date: 1 August 2019

Accepted Date: 9 August 2019

Please cite this article as: Jesús. Ceballos-Torres, S. Gómez-Ruiz, M. Fajardo, A.B. Pinar, S. Prashar, Synthesis and characterization of alkenyl and alkyl substituted group 4 metallocene dichloride complexes: Applications in ethylene polymerization, *Journal of Organometallic Chemistry* (2019), doi: <https://doi.org/10.1016/j.jorganchem.2019.120890>.

This is a PDF file of an article that has undergone enhancements after acceptance, such as the addition of a cover page and metadata, and formatting for readability, but it is not yet the definitive version of record. This version will undergo additional copyediting, typesetting and review before it is published in its final form, but we are providing this version to give early visibility of the article. Please note that, during the production process, errors may be discovered which could affect the content, and all legal disclaimers that apply to the journal pertain.

© 2019 Published by Elsevier B.V.

Synthesis and characterization of alkenyl and alkyl substituted group 4 metallocene dichloride complexes: Applications in ethylene polymerization

Jesús Ceballos-Torres ^a, Santiago Gómez-Ruiz ^{a,*}, Mariano Fajardo ^a, Ana B. Pinar ^b, Sanjiv Prashar ^{a,**}

^a *Departamento de Biología y Geología, Física y Química Inorgánica, E.S.C.E.T., Universidad Rey Juan Carlos, 28933 Móstoles, Madrid, Spain*

^b *Paul Scherrer Institute, Forschungsstrasse 111, 5232 Villigen PSI, Switzerland*

* Corresponding author

** Corresponding author

E-mail addresses: santiago.gomez@urjc.es (S. Gómez-Ruiz), sanjiv.prashar@urjc.es (S. Prashar).

Dedicated to the memory of Professor Pascual Royo

Abstract

The alkenyl substituted zirconocene complexes, $[\text{Zr}(\eta^5\text{-C}_5\text{H}_4\{\text{CMeRCH}_2\text{CH}_2\text{CH}=\text{CMe}_2\})_2\text{Cl}_2]$ ($\text{R} = \text{Me}$ (**1**), Ph (**2**)) were prepared from the reaction of the lithium derivative $\text{Li}(\text{C}_5\text{H}_4\{\text{CMeRCH}_2\text{CH}_2\text{CH}=\text{CMe}_2\})$ ($\text{R} = \text{Me}$, Ph) with zirconium tetrachloride. The bulky alkyl substituted cyclopentadienyl ligand precursor was prepared as its fulvene derivative $(\text{C}_5\text{H}_4)=\text{CMeCH}_2\text{CHMe}_2$ (**3**) via the reaction of cyclopentadiene with 4-methyl-2-pentanone and then converted to $\text{Li}(\text{C}_5\text{H}_4\{\text{CMe}_2\text{CH}_2\text{CHMe}_2\})$ (**4**) via nucleophilic attack of LiMe . The reaction of **4** with $[\text{TiCl}_4(\text{THF})_2]$ and ZrCl_4 gave the metallocene complexes $[\text{M}(\eta^5\text{-C}_5\text{H}_4\{\text{CMe}_2\text{CH}_2\text{CHMe}_2\})_2\text{Cl}_2]$ ($\text{M} = \text{Ti}$ (**5**), Zr (**6**)), respectively. The *ansa*-ligand precursor, $\text{SiMe}_2(\text{C}_5\text{HMe}_4)(\text{C}_5\text{H}_4\{\text{CMe}_2\text{CH}_2\text{CHMe}_2\})$ (**7**), was prepared via the reaction of **4** with $\text{SiMe}_2(\text{C}_5\text{HMe}_4)\text{Cl}$ and subsequently converted to its dilithium derivate, $\text{Li}_2(\text{Me}_2\text{Si}(\text{C}_5\text{Me}_4)(\text{C}_5\text{H}_3\{\text{CMe}_2\text{CH}_2\text{CHMe}_2\}))$ (**8**), using *n*-butyllithium. The *ansa*-zirconocene complex, $[\text{Zr}\{\text{Me}_2\text{Si}(\eta^5\text{-C}_5\text{Me}_4)(\eta^5\text{-C}_5\text{H}_3\{\text{CMe}_2\text{CH}_2\text{CHMe}_2\})\}\text{Cl}_2]$ (**9**), was synthesized by the reaction of **8** with zirconium tetrachloride. Compounds **1-9** were characterized by ^1H and $^{13}\text{C}\{^1\text{H}\}$ NMR spectroscopy. In addition, the molecular structures of **5**, **6** and **9** were determined by single crystal X-ray diffraction studies. The metallocene complexes have been tested as catalyst (with co-catalyst MAO) in the polymerization of ethylene where the substituents on the cyclopentadienyl ligand have a direct influence on the catalytic activity.

Keywords: Titanocene; Zirconocene; *ansa*-Zirconocene; X-ray Crystal Structures; Catalysis; Ethylene Polymerization.

1. Introduction

Metallocene complexes are a very interesting class of compounds with multiple applications in various fields of research such as structural chemistry [1,2], medicinal chemistry [3], organic synthesis [4] and catalysis [5].

In particular, group 4 metallocene complexes are well known as olefin polymerization catalysts [6–8]. They act as single site catalysts producing generally lineal and uniform low polydispersity polyolefins. The metallocene structure has been shown to be directly related to the physical properties of the polyethylene produced. Thus, changing the substituents on the cyclopentadienyl ring and / or the introduction of an *ansa*-bridging unit has been extensively studied. Our group has reported a wide number of group 4 metallocene complexes with interesting applications in olefin polymerization and design of made-to-measure polymers [9–14].

In spite of current environmental problems associated with the use of polyolefins in daily life applications [15], the current needs of the polyolefin industry is still high [16,17] so that the development of novel metallocene catalysts and the research focused on the understanding of the olefin polymerization mechanism are still ongoing [18–20].

Previous studies of our group have demonstrated promising catalytic properties of group 4 metallocene complexes containing different bulky groups or long chain alkyl or alkenyl substituents in the cyclopentadienyl ring [12–14,21,22]. In this context, we present here the synthesis, characterization and catalytic studies in olefin polymerization of group 4 metallocene dichloride complexes incorporating bulky alkyl and alkenyl substituted cyclopentadienyl ligands.

2. Experimental

2.1. General manipulations

All reactions were performed using standard Schlenk tube techniques in an atmosphere of dry nitrogen. Solvents were distilled from the appropriate drying agents and degassed before use. Cyclopentadiene dimer, pyrrolidine, LiBu^n (1.6 M in hexane), LiMe (1.6 M in Et_2O), 4-methyl-2-pentanone, ZrCl_4 and $[\text{TiCl}_4(\text{THF})_2]$ were purchased from Aldrich and used directly. $\text{Li}(\text{C}_5\text{H}_4\{\text{CMe}_2\text{CH}_2\text{CH}_2\text{CH}=\text{CMe}_2\})$ [23], $\text{Li}(\text{C}_5\text{H}_4\{\text{CMePhCH}_2\text{CH}_2\text{CH}=\text{CMe}_2\})$ [24] and $\text{SiMe}_2(\text{C}_5\text{HMe}_4)\text{Cl}$ [25] were synthesized as previously described by us. IR spectra were recorded on a Thermo Nicolet Avatar 330 FT-IR spectrophotometer. ^1H NMR and $^{13}\text{C}\{^1\text{H}\}$ NMR spectra were recorded on a Varian Mercury FT-400 spectrometer. FTIR and NMR spectra of the compounds can be found in the supplementary data. Microanalyses were carried out with a Perkin-Elmer 2400 microanalyzer. Polymer molecular weights and distribution were determined by GPC (Waters 150C Plus or Alliance GPC-2000) in 1,2,4-trichlorobenzene at 150 °C, using standard polystyrene calibration.

2.2. Synthesis of compounds

[Zr(η^5 -C₅H₄{CMe₂CH₂CH₂CH=CMe₂})₂Cl₂] (1): A solution of Li(C₅H₄{CMe₂CH₂CH₂CH=CMe₂}) (0.77 g, 3.96 mmol) in THF (50 mL) was added dropwise during 10 minutes to a solution of ZrCl₄ (0.46 g, 1.98 mmol) in THF (50 mL) at 0 °C. The reaction mixture was allowed to warm to room temperature and stirred for 2–3 h. Solvent was then removed in vacuum and a toluene-hexane 9:1 mixture (50 mL) added to the resulting solid. The suspension was filtered to remove LiCl and the filtrate concentrated (20 mL) and cooled to -30 °C to give the title compound as a pale yellow solid. Yield: 0.56 g, 52 %. FT-IR (KBr): $\bar{\nu}$ 1631 (C=C), 2923, 2964 (C_{al}-H) and 3087, 3101 (C_{ar}-H) cm⁻¹. ¹H NMR (400 MHz, CDCl₃, 25 °C): δ 1.37 (s, 12 H, CpCMe₂), 1.43, 1.65 (m, 4 H each, CH₂CH₂CH=CMe₂), 1.48, 1.62 (s, 6 H each, CH₂CH₂CH=CMe₂), 4.97 (m, 2 H, CH₂CH₂CH=CMe₂) and 6.31, 6.40 (m, 4 H, C₅H₄) ppm. ¹³C{¹H} NMR (100 MHz, CDCl₃, 25 °C): δ 17.7, 23.4 (CH₂CH₂CH=CMe₂), 25.9, 27.1 (CH₂CH₂CH=CMe₂), 36.7 (CpCMe₂), 47.4 (CpCMe₂), 112.7, 116.4, 143.3 (C₅H₄), 124.5 (CH₂CH₂CH=CMe₂) and 131.6 (CH₂CH₂CH=CMe₂) ppm. Elemental analysis calcd (%) for C₂₈H₄₂Cl₂Zr (540.76 g/mol): C 62.19, H 7.83; found: C 61.77, H 7.82.

[Zr(η^5 -C₅H₄{CMePhCH₂CH₂CH=CMe₂})₂Cl₂] (2): The synthesis of **2** was carried out in an identical manner to **1**: Li(C₅H₄{CMePhCH₂CH₂CH=CMe₂}) (0.97 g, 3.76 mmol) and ZrCl₄ (0.44 g, 1.88 mmol). Yield: 0.18 g, 14 %. FT-IR (KBr): $\bar{\nu}$ 1633 (C=C) and 2922 (C_{al}-H) cm⁻¹. ¹H NMR (400 MHz, CDCl₃, 25 °C, for the two isomers): δ 1.44, 1.45, 1.63, 1.63 (s, 6 H each, CH₂CH₂CH=CMe₂), 1.81, 1.82 (s, 6 H each, CpCMePh), 1.50–1.70 (m, 8 H, CH₂CH₂CH=CMe₂), 1.90–2.10 (m, 8 H, CH₂CH₂CH=CMe₂), 5.03 (m, 4 H, CH₂CH₂CH=CMe₂), 5.28, 5.52, 5.96, 5.99, 6.05, 6.14, 6.37, 6.47 (m, 2 H each, C₅H₄) and 7.10–7.40 (m, 20 H, C₆H₅) ppm. ¹³C{¹H} NMR (100 MHz, CDCl₃, 25 °C, for the two isomers): δ 17.8, 23.3, 23.4, 23.6, 24.4, 25.9, 29.9, 32.6, 42.8, 43.6, 43.7, 43.8 (CMePhCH₂CH₂CH=CMe₂) and 109.0, 111.2, 115.4, 116.5, 117.5, 117.6, 119.5, 124.3, 124.4, 126.4, 126.5, 126.5, 127.3, 127.4, 127.5, 128.4, 128.4, 128.5, 131.9, 133.2, 142.5, 142.7, 146.4, 146.5 (CMePhCH₂CH₂CH=CMe₂ and C₅H₄) ppm. Elemental analysis calcd (%) for C₃₈H₄₆Cl₂Zr (664.90 g/mol): C 68.64, H 6.97; found: C 68.24, H 6.83.

(C₅H₄)=CMeCH₂CHMe₂ (3): The synthesis of **3** was carried out in an identical manner to procedure described by Stone and Little [26] using freshly cracked cyclopentadiene (32.95 g, 500 mol), 4-methyl-2-pentanone (20.00 g, 200 mmol), pyrrolidine (21.60 g, 300 mmol) and acetic acid (19.20 g, 320 mmol). Finally, the product was purified by column chromatography using hexane as eluent. Yield: 20.35 g, 69 %. FT-IR (KBr): $\bar{\nu}$ 1638 (C=C), 2869, 2957 (C_{al}-H) and 3069, 3103 (C_{ar}-H) cm⁻¹. ¹H NMR (400 MHz, CDCl₃, 25 °C): δ 1.00 (d, 6 H, CHMe₂), 2.02 (m, 1 H, CHMe₂), 2.25 (s, 3 H, Cp=CMe), 2.48 (d, 2 H, CH₂CHMe₂) and 6.56 (m, 4 H, C₅H₄) ppm. ¹³C{¹H} NMR (100 MHz, CDCl₃, 25 °C): δ 21.4 (Cp=CMe), 23.1 (CHMe₂), 28.1 (CHMe₂), 46.2 (CH₂CHMe₂) and 120.9, 121.1, 130.6, 131.0, 143.8, 153.2 (C₅H₄ and Cp=C) ppm.

Li(C₅H₄{CMe₂CH₂CHMe₂}) (4): LiMe (23.23 mL, 37.16 mmol, 1.60 M in diethyl ether) was added dropwise to (C₅H₄)=CMeCH₂CHMe₂ (**3**) (5.00 g, 33.78 mmol) at 0 °C. The reaction

mixture was allowed to warm to room temperature and stirred for 4 h. The solvent was removed *in vacuo* and the resulting white solid washed with hexane (2 × 50 mL) and dried under vacuum to yield a free-flowing off white powder. Yield: 4.87 g, 97 %. ^1H NMR (400 MHz, $\text{d}_8\text{-THF}$, 25 °C): δ 0.68 (d, 6 H, CHMe_2), 1.19 (s, 6 H, CpCMe_2), 1.37 (d, 2 H, CH_2CHMe_2), 1.55 (m, 1 H, CHMe_2) and 5.48 (m, 4 H, C_5H_4) ppm. $^{13}\text{C}\{^1\text{H}\}$ NMR (100 MHz, $\text{d}_8\text{-THF}$, 25 °C): δ 26.8 (CHMe_2), 27.0 (CHMe_2), 32.9 (CpCMe_2), 36.9 (CH_2CHMe_2), 57.5 (CpCMe_2) and 102.2, 102.9, 130.6 (C_5H_4) ppm.

$[\text{Ti}(\eta^5\text{-C}_5\text{H}_4\{\text{CMe}_2\text{CH}_2\text{CHMe}_2\})_2\text{Cl}_2]$ (5): The synthesis of **5** was carried out in an identical manner to **1**: $\text{Li}(\text{C}_5\text{H}_4\{\text{CMe}_2\text{CH}_2\text{CHMe}_2\})$ (2.00 g, 11.77 mmol) and $[\text{TiCl}_4(\text{THF})_2]$ (1.97 g, 5.89 mmol). Yield 0.51 g, 26 %. FT-IR (KBr): $\bar{\nu}$ 2867, 2922, 2954 ($\text{C}_{\text{al}}\text{-H}$) and 3089 ($\text{C}_{\text{ar}}\text{-H}$) cm^{-1} . ^1H NMR (400 MHz, CDCl_3 , 25 °C): δ 0.70 (d, 12 H, CHMe_2), 1.37 (s, 12 H, CpCMe_2), 1.39 (d, 4 H, CH_2CHMe_2), 1.42 (m, 2 H, CH_2CHMe_2) and 6.46, 6.54 (m, 4 H each, C_5H_4) ppm. $^{13}\text{C}\{^1\text{H}\}$ NMR (100 MHz, CDCl_3 , 25 °C): δ 24.6 (CHMe_2), 25.3 (CHMe_2), 27.5 (CpCMe_2), 38.0 (CH_2CHMe_2), 56.7 (CpCMe_2) and 117.6, 120.5, 149.0 (C_5H_4) ppm. Elemental analysis calcd (%) for $\text{C}_{24}\text{H}_{38}\text{Cl}_2\text{Ti}$ (445.33 g/mol): C 64.73, H 8.60; found: C 65.02, H 8.87.

$[\text{Zr}(\eta^5\text{-C}_5\text{H}_4\{\text{CMe}_2\text{CH}_2\text{CHMe}_2\})_2\text{Cl}_2]$ (6): The synthesis of **6** was carried out in an identical manner to **1**: $\text{Li}(\text{C}_5\text{H}_4\{\text{CMe}_2\text{CH}_2\text{CHMe}_2\})$ (**4**) (1.50 g, 8.83 mmol) and ZrCl_4 (1.03 g, 4.41 mmol). Yield: 0.65 g, 63 %. FT-IR (KBr): $\bar{\nu}$ 2862, 2925, 2957 ($\text{C}_{\text{al}}\text{-H}$) cm^{-1} . ^1H NMR (400 MHz, CDCl_3 , 25 °C): δ 0.68 (d, 12 H, CHMe_2), 1.37 (s, 12 H, CpCMe_2), 1.38 (d, 4 H, CH_2CHMe_2), 1.40 (m, 2 H, CH_2CHMe_2) and 6.31, 6.41 (m, 4 H each, C_5H_4) ppm. $^{13}\text{C}\{^1\text{H}\}$ NMR (100 MHz, CDCl_3 , 25 °C): δ 24.6 (CHMe_2), 25.2 (CHMe_2), 27.8 (CpCMe_2), 37.0 (CH_2CHMe_2), 56.5 (CpCMe_2) and 112.7, 116.5, 143.8 (C_5H_4) ppm. Elemental analysis calcd (%) for $\text{C}_{24}\text{H}_{38}\text{Cl}_2\text{Zr}$ (488.69 g/mol): C 58.99, H 7.84; found: C 58.90, H 7.97.

$\text{SiMe}_2(\text{C}_5\text{HMe}_4)(\text{C}_5\text{H}_4\{\text{CMe}_2\text{CH}_2\text{CHMe}_2\})$ (7): A solution of **4** (2.00 g, 11.77 mmol) in THF (50 mL) was added dropwise to a solution of $\text{SiMe}_2(\text{C}_5\text{HMe}_4)\text{Cl}$ (2.53 g, 11.79 mmol) in THF (50 mL) at -80 °C. The reaction mixture was allowed to warm to room temperature and stirred for 24 hours. The solvent was then removed in vacuum and hexane (50 mL) was added to the resulting orange oil. The mixture was filtered and the solvent removed under reduced pressure to give an orange oil. Yield: 3.77 g, 83 %. ^1H NMR (400 MHz, CDCl_3 , 25 °C, for the predominant isomer): δ -0.16 (s, 6 H, SiMe_2), 0.82, 0.86 (d, 3 H each, CHMe_2), 1.16, 1.17 (s, 3 H each, CpCMe_2), 1.42 (d, 2 H, CH_2CHMe_2), 1.54 (m, 1 H, CHMe_2), 1.86, 2.00 (s, 6 H each, C_5Me_4), 2.93, 3.19 (s, 1 H each, HC_5Me_4 and HC_5H_3) and 5.90, 6.30, 6.57 (m, 1 H each, HC_5H_3) ppm. $^{13}\text{C}\{^1\text{H}\}$ NMR (100 MHz, CDCl_3 , 25 °C, for the predominant isomer): δ 1.0 (SiMe_2), 24.9, 25.0 (CHMe_2), 28.5, 29.5 (CpCMe_2), 35.7 (CHMe_2), 36.9 (CpCMe_2), 40.5, 41.0 (C_5Me_4), 51.3 (CH_2CHMe_2), 52.9 ($\text{C}^1\text{-C}_5\text{Me}_4$), 68.2 ($\text{C}^1\text{-C}_5\text{H}_3$) and 123.7, 125.0, 130.6, 132.2, 133.2, 133.3, 156.0, 158.8 (C_5H_3 and C_5Me_4) ppm.

$\text{Li}_2(\text{Me}_2\text{Si}(\eta^5\text{-C}_5\text{Me}_4)(\text{C}_5\text{H}_3\{\text{CMe}_2\text{CH}_2\text{CHMe}_2\}))$ (8): A solution of LiBu^n (8.82 mL, 22.05 mmol, 2.50 M in hexane) was added dropwise to a solution of **7** (3.77 g, 11.02 mmol) in hexane (50 mL) at -80°C . The reaction mixture was allowed to warm to room temperature and stirred for 24 hours. The solvent was then removed in vacuum and the resulting solid washed with hexane (2×50 mL) and finally dried in vacuum. Yield: 3.45 g, 91 %. ^1H NMR (400 MHz, $\text{d}_8\text{-THF}$, 25°C): δ 0.39 (s, 6 H, SiMe_2), 0.76, 0.78 (s, 3 H each, CpCMe_2), 1.18 (s, 6 H, CHMe_2), 1.42 (d, 2 H, CH_2CHMe_2), 1.60 (m, 1 H, CHMe_2), 1.90, 2.07 (s, 6 H each, C_5Me_4) and 5.68, 5.77, 5.83 (m, 1 H each, C_5H_3) ppm. $^{13}\text{C}\{^1\text{H}\}$ NMR (100 MHz, $\text{d}_8\text{-THF}$, 25°C): δ 4.8 (SiMe_2), 11.6, 14.8 (C_5Me_4), 25.8 (CHMe_2), 26.0 (CHMe_2), 31.8 (CH_2CHMe_2), 36.0 (CpCMe_2), 56.1 (CpCMe_2) and 103.6, 108.2, 110.4, 111.5, 113.4, 116.4, 129.7, 132.81 (C_5H_3 and C_5Me_4) ppm.

$[\text{Zr}(\text{Me}_2\text{Si}(\eta^5\text{-C}_5\text{Me}_4)(\eta^5\text{-C}_5\text{H}_3\{\text{CMe}_2\text{CH}_2\text{CHMe}_2\}))\text{Cl}_2]$ (9): The synthesis of **9** was carried out in an identical manner to **1**: $\text{Li}_2(\text{Me}_2\text{Si}(\eta^5\text{-C}_5\text{Me}_4)(\text{C}_5\text{H}_3\{\text{CMe}_2\text{CH}_2\text{CHMe}_2\}))$ (**8**) (3.45 g, 9.75 mmol) and ZrCl_4 (2.27 g, 9.75 mmol). Yield: 0.43 g, 9 %. FT-IR (KBr): $\bar{\nu}$ 803 (Si–C stretching), 1259 (Si–CH₃ sym bending) and 2873, 2927, 2960 ($\text{C}_{\text{al}}\text{--H}$) cm^{-1} . ^1H NMR (400 MHz, CDCl_3 , 25°C): δ 0.63 (d, 6 H, CHMe_2), 0.81, 0.85 (s, 3 H each, SiMe_2), 0.83 (d, 2 H, CH_2CHMe_2), 1.41, 1.48 (s, 3 H each, CpCMe_2), 1.48 (m, 1 H, CH_2CHMe_2), 1.90, 1.98, 2.00, 2.03 (s, 3 H each, C_5Me_4) and 5.57, 5.66, 6.85 (m, 1 H each, C_5H_3) ppm. $^{13}\text{C}\{^1\text{H}\}$ NMR (100 MHz, CDCl_3 , 25°C): δ -0.4, 0.4 (SiMe_2), 12.2, 12.5 (CpCMe_2), 15.2 (CHMe_2), 24.3, 25.0, 25.1, 25.6 (C_5Me_4), 28.3 (CHMe_2), 37.0 (CH_2CHMe_2), 56.2 (CpCMe_2), 97.7, 104.2 ($\text{C}^1\text{--Cp}$), 111.6, 124.0, 127.1, 150.9 (C_5H_3) and 113.7, 127.6, 135.2, 136.5 (C_5Me_4) ppm. Elemental analysis calcd (%) for $\text{C}_{23}\text{H}_{36}\text{Cl}_2\text{SiZr}$ (502.75 g/mol): C 54.95, H 7.22; found: C 54.83, H 7.05.

2.3. Data collection and structural refinement of **5**, **6** and **9**

Data were collected with an Oxford Gemini CCD system ($\lambda(\text{MoK}\alpha) = 0.71073 \text{ \AA}$, $T = 293(2) \text{ K}$) using ω and ψ scans. Semi-empirical from equivalents absorption corrections were carried out with SCALE3 ABSPACK [27]. The structures were solved by direct methods [28]. Structure refinements were carried out with SHELXL-97 [29]. All non-hydrogen atoms were refined anisotropically and H atoms were refined using the riding model. Table 1 lists crystallographic details.

Table 1. Crystallographic data of **5**, **6** and **9**

Compound	5	6	9
Empirical formula	$\text{C}_{24}\text{H}_{38}\text{Cl}_2\text{Ti}$	$\text{C}_{24}\text{H}_{38}\text{Cl}_2\text{Zr}$	$\text{C}_{23}\text{H}_{36}\text{Cl}_2\text{SiZr}$
Molecular weight (g/mol)	445.34	488.66	502.73
Temperature (K)	293(2)	293(2)	293(2)
Wavelength (Å)	0.71073	0.71073	0.71073
Crystal system	Monoclinic	Monoclinic	Triclinic
Space group	C2/c	C2/c	$P-1$

a (pm)	2888.65(18)	2901.02(4)	959.80(2)
b (pm)	665.39(3)	670.320(10)	1020.50(2)
c (pm)	1389.77(7)	1396.86(2)	1487.90(2)
α ($^\circ$)	90.00	90.00	72.9040(10)
β ($^\circ$)	111.149(6)	111.845(2)	71.6270(10)
γ ($^\circ$)	90.00	90.00	66.508(2)
Volume (\AA^3)	2.4913(2)	2521.30(6)	1244.49(4)
Z	4	4	2
Calculated density (mg/m^3)	1.187	1.287	1.342
Absorption coefficient μ (mm^{-1})	0.564	0.655	0.711
F(000)	952	1024	524
Crystal size (mm)	0.2x0.1x0.05	0.40x0.20x0.04	0.30x0.20x0.20
θ range ($^\circ$)	4.26 a 25.67	4.21 a 29.60	4.17 a 29.53
<i>hkl</i> ranges	-34 $\leq h \leq$ 34 -8 $\leq k \leq$ 8 -16 $\leq l \leq$ 16	-40 $\leq h \leq$ 39 -9 $\leq k \leq$ 9 -19 $\leq l \leq$ 18	-11 $\leq h \leq$ 11 -12 $\leq k \leq$ 12 -18 $\leq l \leq$ 18
Collected reflections	64215	98791	70549
Independent reflections	2347 [R _(int) = 0.1653]	3472 [R _(int) = 0.0221]	5065 [R _(int) = 0.0331]
Completeness	99.5 % ($\theta = 25.67^\circ$)	97.4 % ($\theta = 29.60^\circ$)	99.6 % ($\theta = 29.53^\circ$)
Maximum and minimum transition	1.000 and 0.93502	1.0000 and 0.88308	1.0000 and 0.97773
Refinement method	Least squares on F ²	Least squares on F ²	Least squares on F ²
Data / Restraints / Parameters	2347 / 0 / 123	3472 / 0 / 123	5065 / 0 / 263
Goodness-of-fit on F²	1.016	1.039	1.044
Final R indices [$I > 2\sigma(I)$]	R ₁ = 0.0671 wR ₂ = 0.1702	R ₁ = 0.0270 wR ₂ = 0.0727	R ₁ = 0.0395 wR ₂ = 0.1088
Final R indices (all data)	R ₁ = 0.1347 wR ₂ = 0.2157	R ₁ = 0.0296 wR ₂ = 0.0752	R ₁ = 0.0452 wR ₂ = 0.1148
Largest diffraction peak and hole ($\text{e} \cdot \text{\AA}^{-3}$)	0.492 and -0.210	0.670 and -0.308	0.875 and -0.299

2.4 Polymerization

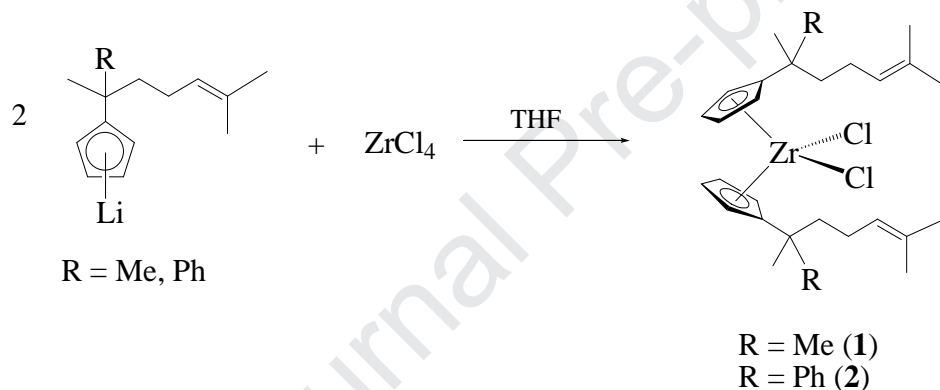
The temperature of a 1 litre glass autoclave was set to 10, 40 or 80 °C. Under an inert N₂ atmosphere, the metallocene catalyst (7.5 μmol), MAO (quantity to obtain a Al/M 1000:1 ratio) and toluene (200 mL) were mixed together for 15 min. The N₂ pressure inside the autoclave

was reduced by applying vacuum. Ethylene pressure of 2 bar was then applied and maintained to the autoclave and stirring of the mixture commenced (1000 rpm). After exactly 60 minutes, stirring was stopped and the ethylene pressure released. Excess MAO was then destroyed by adding a mixture of MeOH/HCl (9:1). The polymer was isolated by filtration and washed with ethanol and dried under vacuum at 90 °C for 24 h.

3. Results and discussion

3.1 Synthesis and characterization of alkenyl-substituted zirconocene complexes **1** and **2**

The complexes $[\text{Zr}(\eta^5\text{-C}_5\text{H}_4\{\text{CMeRCH}_2\text{CH}_2\text{CH}=\text{CMe}_2\})_2\text{Cl}_2]$ (R = Me (**1**), Ph (**2**)) have been synthesized by the reaction of two molar equivalents of the corresponding lithium derivative $\text{Li}(\text{C}_5\text{H}_4\{\text{CMeRCH}_2\text{CH}_2\text{CH}=\text{CMe}_2\})$ (R = Me, Ph) with one molar equivalent of ZrCl_4 in THF for 3 hours at room temperature (Scheme 1). **1** and **2** were isolated as pale yellow solids



Scheme 1. Synthesis of alkenyl-substituted zirconocene complexes **1** and **2**

1 and **2** were characterized by IR spectroscopy. For the alkenyl groups, vibration bands corresponding to the stretching of the C–H bonds of the alkenyl substituent and in the case of **2** aromatic groups around 2900–3100 cm^{-1} were recorded. Furthermore, a band close to 1630 cm^{-1} was assigned to the stretching vibration of C=C double bonds.

Characterization by ^1H NMR spectroscopy showed the expected signals in each case due to the different groups of protons in the molecule (see Experimental section). In the spectrum of **1**, two multiplets at 6.31 and 6.40 ppm, assigned to the two types of magnetically equivalent protons of the monosubstituted cyclopentadienyl ligands, were observed. Moreover, the expected signals for the alkenyl fragment were also present: a singlet at 1.37 ppm corresponding to the twelve protons of the four equivalent methyl groups, two singlets at 1.48 and 1.62 ppm assigned to the protons of the four terminal methyl groups of the alkenyl substituent and two multiplets at 1.43 and 1.65 ppm due to the protons of the four methylene groups. Finally, a multiplet at 4.97 ppm was assigned to the two protons bonded to the sp^2 carbon atoms.

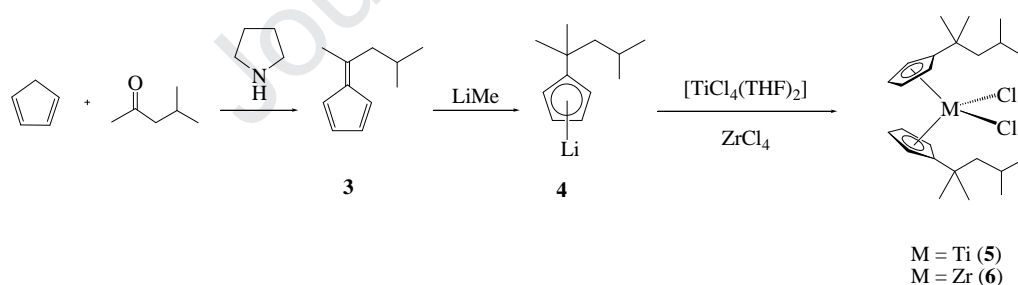
The ^1H NMR spectrum of **2** reveals the presence of two diastereomers (*meso* and *rac* isomers) in a ratio of approximately 1:1 as a consequence of the presence of two chiral carbon atoms in this molecule.

In the $^{13}\text{C}\{^1\text{H}\}$ NMR spectrum of **1**, the expected signals due to the alkenyl fragment and the cyclopentadienyl rings were observed (see Experimental section): two signals at 17.7 and 23.4 ppm due to the two carbon atoms of the terminal methyl groups of the alkenyl substituent, two additional signals corresponding to the two carbon atoms of the methylene groups at 25.9 and 27.1 ppm, another signal assigned to the two equivalent methyl groups at 36.7 ppm. A signal around 47 ppm due to the quaternary carbon atom bonded directly to the cyclopentadienyl ring was also observed. The signals corresponding to the sp^2 carbon atoms of the C=C double bond were located at 124.5 and 131.6 ppm, whereas the three carbon atoms of the cyclopentadienyl ring were recorded at 112.7, 116.4 and 143.3 ppm.

The $^{13}\text{C}\{^1\text{H}\}$ NMR spectrum of **2** again confirms the presence of two isomers as a consequence of two chiral carbon atoms in the molecule (see Experimental section).

3.2 Synthesis and characterization of bulky alkyl-substituted group 4 metallocene complexes **5** and **6**

The metallocene complexes, $[\text{M}(\eta^5\text{-C}_5\text{H}_4\{\text{CMe}_2\text{CH}_2\text{CHMe}_2\})_2\text{Cl}_2]$ ($\text{M} = \text{Ti}$ (**5**), Zr (**6**)), were synthesized in a multi-step process (Scheme 2). Initially, the synthesis of 6-isobutyl-6-methylfulvene (**3**) was carried out according to the method described by Little and coworkers [26]. **3** was purified by liquid-liquid extraction with ether and by column chromatography using hexane as eluent.



Scheme 2. Synthetic route to bulky alkyl-substituted group 4 metallocene complexes **5** and **6**

The IR spectrum of **3** showed the band corresponding to the stretching vibration of C=C double bond at 1638 cm^{-1} , and those assigned to the stretching vibration of C—H bonds at 2869 and 2957 cm^{-1} (for $\text{C}_{\text{al}}\text{—H}$) and 3069 and 3103 cm^{-1} (for $\text{C}_{\text{ar}}\text{—H}$).

In the ^1H NMR spectrum of **3** a set of four signals due to the protons located on the aliphatic carbon atoms was observed along with a doublet at 1.00 ppm assigned to the two terminal methyl groups, a multiplet at 2.02 ppm due to the proton located on the tertiary carbon atom, a singlet at 2.25 ppm corresponding to the methyl group situated on the end of the alkyl chain and, finally, a doublet at 2.48 ppm assigned to the two protons of the methylene group. In

addition to these signals, a multiplet at 6.56 ppm corresponding to the protons located on the sp^2 carbon atoms of the cyclopentadiene ring was also observed.

The $^{13}\text{C}\{^1\text{H}\}$ NMR spectrum showed the expected signals for the different carbon atoms. Thus, four signals between 20 and 50 ppm corresponding to the sp^3 carbon atoms were observed, while for the sp^2 carbon atoms there were six additional signals between 120 to 160 ppm.

In the subsequent synthetic step, the reaction of **3** with LiMe gave the corresponding lithium derivative $\text{Li}(\text{C}_5\text{H}_4\{\text{CMe}_2\text{CH}_2\text{CHMe}_2\})$ (**4**) as a highly air-sensitive white powder. The ^1H and $^{13}\text{C}\{^1\text{H}\}$ NMR spectra of **4** are very similar to those obtained for compound **3** (see Experimental section).

The reaction of 2 molar equivalents of **4** with $[\text{TiCl}_4(\text{THF})_2]$ and ZrCl_4 gave the metallocene complexes $[\text{M}(\eta^5\text{-C}_5\text{H}_4\{\text{CMe}_2\text{CH}_2\text{CHMe}_2\})_2\text{Cl}_2]$ ($\text{M} = \text{Ti}$ (**5**), Zr (**6**)), respectively.

The IR spectra of **5** and **6** showed the expected bands due to the different vibration modes of the molecule, of special importance is the band corresponding to the stretching vibration of the $\text{C}_{\text{ar}}\text{--H}$ bond of the alkyl fragment and the cyclopentadienyl at ca. 3000 cm^{-1} . (see Experimental section). In the ^1H NMR spectrum of **5**, the expected signals of the alkyl fragment were observed: a doublet at 0.70 ppm assigned to the protons of the two terminal methyl groups of the alkyl substituents bonded to both cyclopentadienyl rings, a singlet at 1.37 ppm due to the protons of the two equivalent methyl groups situated on the quaternary carbon atom, another doublet at 1.39 ppm for the protons of the methylene group and a multiplet at 1.42 ppm corresponding to the proton bonded to the tertiary carbon atom. In addition to these signals, two multiplets at 6.46 and 6.54 ppm assigned to the aromatic protons of the cyclopentadienyl rings were also observed.

In the $^{13}\text{C}\{^1\text{H}\}$ NMR spectrum of **5**, the five signals assigned to the sp^3 carbon atoms of the alkyl substituent, as well as the corresponding three signals due to the carbon atoms of the aromatic cyclopentadienyl rings were recorded (see Experimental section). The ^1H and $^{13}\text{C}\{^1\text{H}\}$ NMR spectra of **6** are very similar to those obtained for compound **5** (see Experimental section).

3.3. X-ray Crystal Structures of $[\text{Ti}(\eta^5\text{-C}_5\text{H}_4\{\text{CMe}_2\text{CH}_2\text{CHMe}_2\})_2\text{Cl}_2]$ (**5**) and $[\text{Zr}(\eta^5\text{-C}_5\text{H}_4\{\text{CMe}_2\text{CH}_2\text{CHMe}_2\})_2\text{Cl}_2]$ (**6**)

The molecular structures of the metallocene complexes **5** and **6** were determined by single-crystal X-ray diffraction studies (Figures 1 and 2). **5** and **6** crystallize in the monoclinic C2/c space group, with four molecules in unit cell ($Z = 4$) and only half of the molecule in the asymmetric unit because of the presence of a symmetry plane. Selected bond angles and lengths are given in Table 2.

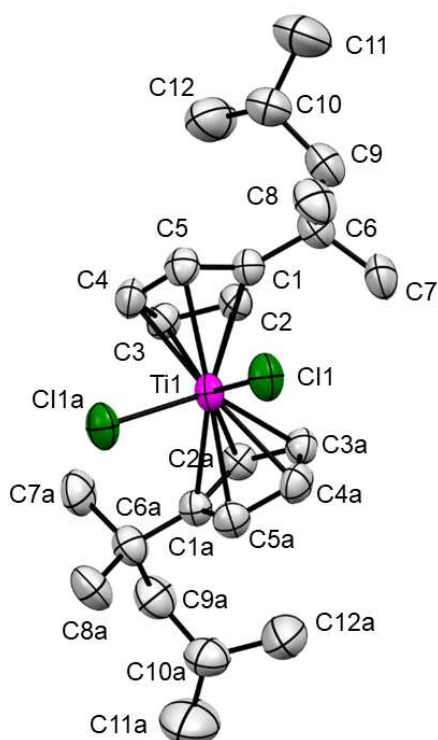


Figure 1. Molecular structure and atom-labelling scheme for **5** with ellipsoids at 30% probability (hydrogen atoms are omitted for clarity)

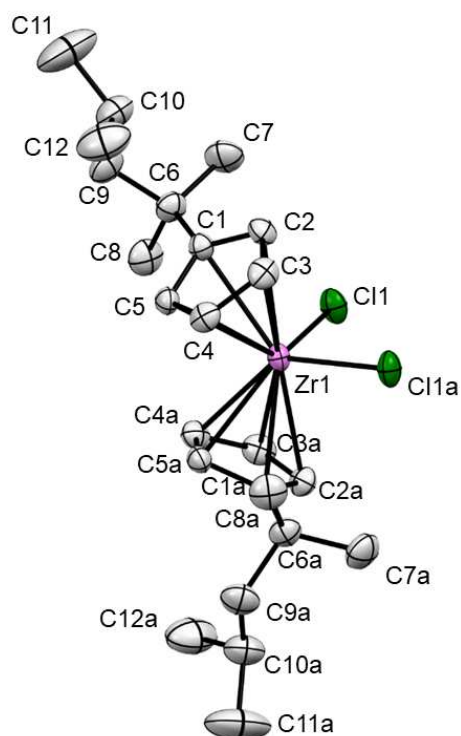


Figure 2. Molecular structure and atom-labelling scheme for **6** with ellipsoids at 30% probability (hydrogen atoms are omitted for clarity)

Table 2. Selected Bond Lengths (Å) and Angles (°) for **5** and **6**^a

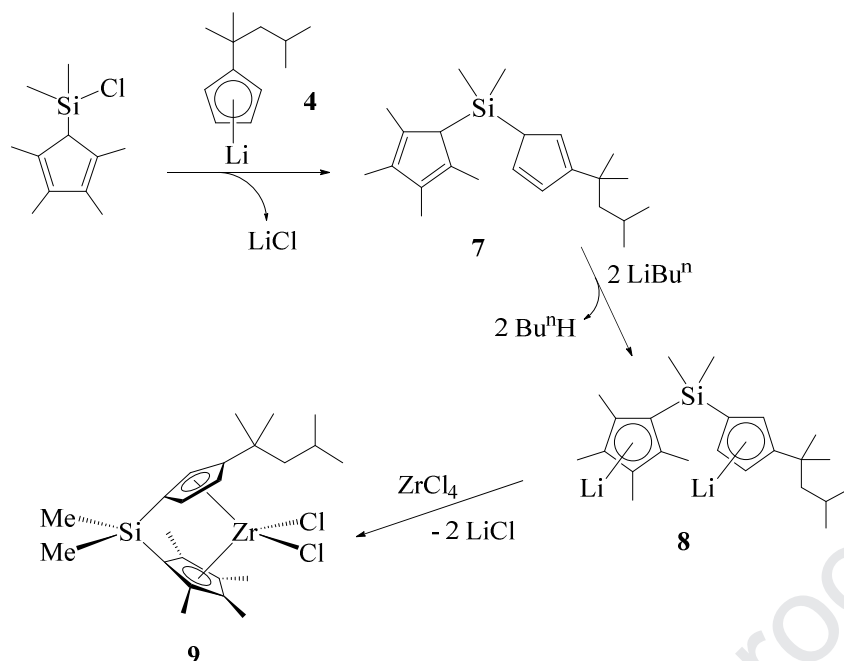
	5	6
M1–Cent	2.083(9)	2.218(8)
M1–Cl1	2.367(2)	2.445(2)
C1–C2	1.399(6)	1.416(2)
C2–C3	1.412(6)	1.408(2)
C3–C4	1.371(6)	1.417(2)
C4–C5	1.401(7)	1.396(3)
C1–C5	1.408(6)	1.406(2)
C1–C6	1.513(8)	1.520(2)
C6–C7	1.532(7)	1.529(3)
C6–C9	1.564(8)	1.554(3)
C9–C10	1.522(8)	1.528(4)
C10–C11	1.494(9)	1.514(4)
C10–C12	1.515(9)	1.511(4)
Cent–M1–Cent	130.9(3)	129.3(4)
Cent–M1–Cl1	106.7(3)	106.3(3)
Cent–M1–Cl1a	107.3(3)	107.9(3)
Cl1–M1–Cl1a	90.67(7)	93.26(2)
C2–C1–C6	125.2(4)	128.3(1)
C2–C3–C4	107.2(4)	109.0(2)
C1–C6–C7	111.2(4)	111.4(2)
C1–C6–C8	111.8(4)	110.6(2)
C1–C6–C9	107.6(4)	108.4(2)
C6–C9–C10	119.4(5)	119.3(2)
C11–C10–C12	109.7(8)	109.7(3)

^a Cent is the centroid of C1–C5 or C1a–C5a.

It should be noted that **5** and **6** are isostructural. Bond distances and angles are similar to those found in other group 4 metallocene complexes published by our research group [13,30–32]. The molecular structures of **5** and **6** present the typical conformation of a bent metallocene with the metal atom situated in a distorted tetrahedral environment (Cent–M1–Cent, Ti 130.9(3)°; Zr 129.3(4)°) with the coordination of the cyclopentadienyl ligands to the metal centre in an η^5 mode and M–Cl bonds of 2.367(2) Å, Ti; 2.445(2) Å, Zr. It is interesting to note that the angle C6–C9–C10 = 119.4(5)°, Ti; 119.3(2)°, Zr, is quite different to that which corresponds to an sp^3 hybridization (for atom C9), which is a consequence of the presence of the terminal isopropyl group. Finally, bond lengths and angles involving the carbon atoms of the cyclopentadienyl ring as well as those of the alkyl substituent confirm their corresponding sp^2 and sp^3 hybridization.

3.4. Synthesis and characterization of bulky alkyl-substituted ansa-metallocene complex [Zr{Me₂Si(η^5 -C₅Me₄)(η^5 -C₅H₃{CMe₂CH₂CHMe₂})}Cl₂] (**9**)

The preparation of compound **9** was carried out through various synthetic steps (Scheme 3).



Scheme 3. Synthetic route for the preparation of **9**.

The addition of $\text{SiMe}_2(\text{C}_5\text{HMe}_4)\text{Cl}$ to a solution of **4** in THF, in a molar ratio of 1:1, led to the formation of the *ansa*-bis(cyclopentadiene) derivative $\text{SiMe}_2(\text{C}_5\text{HMe}_4)(\text{C}_5\text{H}_4\{\text{CMe}_2\text{CH}_2\text{CHMe}_2\})$ (**7**) as a yellow oil which was isolated as a mixture of isomers (Figure 3), and characterized by ^1H NMR and $^{13}\text{C}\{^1\text{H}\}$ NMR spectroscopy.

In the ^1H NMR spectrum of **7** the signals corresponding to the different isomers (Figure 2) are observed. The isomers formed are preferably the 1,3-disubstituted cyclopentadiene derivatives, as a consequence that the nucleophilic attack preferentially occurs in this position and not in the 2 position of the ring due to steric hindrance exerted by the alkyl substituent. Furthermore, there is a predominant isomer which corresponds to isomer **I** (Figure 3) according to the NMR spectrum. This isomer is observed in the mixture in a proportion of about 66 %.

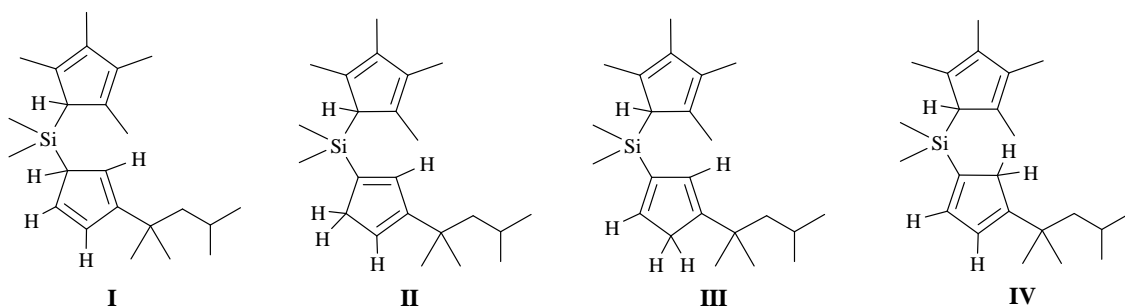


Figure 3. Isomers of the *ansa*-bis(cyclopentadiene) derivative **7**.

In the ^1H NMR spectrum, the signals corresponding to the predominant isomer were: a singlet at -0.16 ppm assigned to the protons of the two methyl groups of the *ansa*-bridge, two

doublets at 0.82 and 0.86 ppm corresponding to the protons of the two non-equivalent terminal methyl groups of the alkyl fragment, two singlets which resonated at a very similar chemical shifts (1.16 and 1.17 ppm) which have been assigned to the protons of the two methyl groups located at the quaternary carbon of the alkyl substituent, a doublet for the protons of the methylene group at around 1.42 ppm, a multiplet at 1.54 ppm due to the methine proton of this substituent and, finally, two singlets due to protons of the four equivalent methyl groups of the tetramethylcyclopentadiene ring. In addition to these signals, two additional singlets at 2.93 and 3.19 ppm corresponding to the two acidic protons of the two cyclopentadiene rings were observed, while olefinic protons of the disubstituted cyclopentadiene ring resonated between 5.90 and 6.60 ppm.

With regards to the characterization by $^{13}\text{C}\{^1\text{H}\}$ NMR spectroscopy, signals were assigned to the predominant isomer. The carbon atoms of the *ansa*-bridge were recorded at 1.0 ppm. In addition, the atoms of the alkyl substituent gave signals from 25 to 53 ppm: the carbon atoms of terminal methyl groups were observed at very similar chemical shifts (24.9 and 25.0 ppm), the carbons of the two methyl groups on the quaternary carbon atom appeared at 28.5 and 29.5 ppm, the carbon atom belonging to methine group has a chemical shift of 35.7 ppm, whereas above 50 ppm the signals due the carbon atom of the methylene group and the quaternary carbon were also observed. The carbon atoms of the four methyl groups of pentasubstituted cyclopentadiene ring were recorded at 40.5 and 41.0 ppm, and the two sp^3 carbon atoms of the cyclopentadiene rings at 52.9 and 68.2 ppm for the di- and penta-substituted ring, respectively. Finally, the olefinic carbon atoms appeared as eight signals between 123 and 159 ppm.

Deprotonation of the two cyclopentadiene rings of **7** was carried out using two equivalents of LiBu^n to give the corresponding lithium derivative **8** (Scheme 3) which was isolated as a highly air-sensitive orange solid.

8 was characterized using ^1H NMR and $^{13}\text{C}\{^1\text{H}\}$ NMR spectroscopy, observing the expected signals due to the protons and carbons of the lithium derivative. The ^1H NMR spectrum of **8** showed the following signals: a singlet at 0.39 ppm assigned to the six protons of the two methyl groups of the *ansa*-bridge, two additional singlets at 0.76 and 0.78 ppm due to the two methyl groups on the quaternary carbon atom of the alkyl chain, one singlet at 1.18 ppm corresponding to the two terminals methyl groups of the alkyl substituent, one doublet due to the methylene group at 1.42 ppm, one multiplet assigned to the methine proton at 1.60 ppm, two singlets for the four methyl groups of the pentasubstituted cyclopentadienyl ring at 1.90 and 2.07 ppm and, finally, three multiplets between 5.68 and 5.83 assigned to the protons of the disubstituted cyclopentadienyl ring.

The $^{13}\text{C}\{^1\text{H}\}$ NMR spectrum confirmed the proposed structure for this di-lithium derivative **8** showing a signal at 4.8 ppm corresponding to the carbon atoms of the two methyl groups of the *ansa*-bridge, two signals assigned to the four methyl groups of the pentasubstituted cyclopentadienyl ring at 11.6 and 14.8 ppm, and five signals between 25.8 and

56.1 ppm due to the carbon atoms of the alkyl substituent of the disubstituted cyclopentadienyl ring. In addition, eight signals for the carbon atoms of the cyclopentadienyl rings were observed.

In the ^1H NMR spectrum of **8** the methyl groups of the C_5Me_4 fragment gave only two peaks as the chemical shifts are identical in the case of C2 with C5 and C3 with C4. The same occurs in the $^{13}\text{C}\{^1\text{H}\}$ NMR spectrum. For the cyclopentadienyl rings, the ten carbon atoms gave eight signals, with the pairs C2 with C5 and C3 with C4 giving one signal each. The methyl groups of the *ansa*-bridge are also equivalent. All this indicates that the dilithium compound does not adopt a rigid structure (as in the *ansa*-zirconocene complex **9**) in solution.

Finally, transmetallation reaction using the lithium derivative **8** and ZrCl_4 was carried out in a molar ratio of 1:1, to obtain the *ansa*-zirconocene complex $[\text{Zr}\{\text{Me}_2\text{Si}(\eta^5\text{-C}_5\text{Me}_4)(\eta^5\text{-C}_5\text{H}_3\{\text{CMe}_2\text{CH}_2\text{CHMe}_2\})\}\text{Cl}_2]$ (**9**) (Scheme 3) as a yellow crystalline solid.

Complex **9** has been characterized by IR, ^1H NMR and $^{13}\text{C}\{^1\text{H}\}$ NMR spectroscopy, elemental analysis and single-crystal X-ray diffraction studies.

In the characterization by IR spectroscopy, bands corresponding to the stretching vibration of the $\text{C}_{\text{al}}\text{-H}$ bonds of the alkyl fragment below 3000 cm^{-1} were observed.

The ^1H NMR spectrum of **9** showed the expected signals. In the case of the alkyl moiety bound to one of the cyclopentadienyl rings, the spectrum shows the following signals: a doublet at 0.63 ppm due to the protons of the two terminal methyl groups, another doublet assigned to the protons of the methylene group at 0.83 ppm, a multiplet at 1.48 ppm corresponding to the proton located on the tertiary carbon atom and two singlets due to the protons of the two methyl groups situated on the quaternary carbon atom directly bonded to the cyclopentadienyl ring. In this case, and in contrast to the compounds **5** and **6**, these methyl groups are diastereotopic because of the presence of planar chirality in the molecule. However, the two terminal methyl groups of the alkyl substituent, as indicated before, gave only one signal as they are somewhat distanced from the source of the planar chirality. This was also observed in the dilithium precursor **8**.

In addition to these signals involving the alkyl substituent, four singlets between 1.90 and 2.10 ppm assigned to the protons of the four methyl groups of the other cyclopentadienyl ring and two singlets about 0.85 ppm, corresponding to the protons of the two methyl groups forming the *ansa*-bridge were observed. Finally, the three protons attached to the substituted cyclopentadienyl ring resonated as three multiplets at 5.57, 5.66 and 6.85 ppm.

Regarding the characterization by $^{13}\text{C}\{^1\text{H}\}$ -NMR, the spectrum of **9** shows two signals around 0 ppm corresponding to the two carbon atoms of the methyl groups attached to the silicon atoms of the *ansa*-bridge, two signals at 12 ppm due to the two carbon atoms of the diastereotopic methyl groups substituting the quaternary carbon atom directly bonded to one of the cyclopentadienyl rings, only one signal for the two terminal methyl groups of the alkyl substituent at 15.2 ppm and three more signals due to the remaining sp^3 carbon atoms of the alkyl substituent.

In addition to these signals, the four carbon atoms of the methyl groups bonded to one of the cyclopentadienyl rings resonated at similar chemical shifts (24.3, 25.0, 25.1 and 25.6

ppm), while towards lower fields, above 100 ppm, ten signals corresponding to the ten carbon atoms of the two cyclopentadienyl rings were observed.

3.5. X-ray Crystal Structure of $[\text{Zr}\{\text{Me}_2\text{Si}(\eta^5\text{-C}_5\text{Me}_4)(\eta^5\text{-C}_5\text{H}_3\{\text{CMe}_2\text{CH}_2\text{CHMe}_2\})\}\text{Cl}_2]$ (**9**)

The molecular structure of the *ansa*-zirconocene complex **9** was determined by single-crystal X-ray diffraction studies (Figure 4). Compound **9** crystallizes in the triclinic *P*-1 space group with two molecules in the unit cell. Selected bond angles and lengths are given in Table 3.

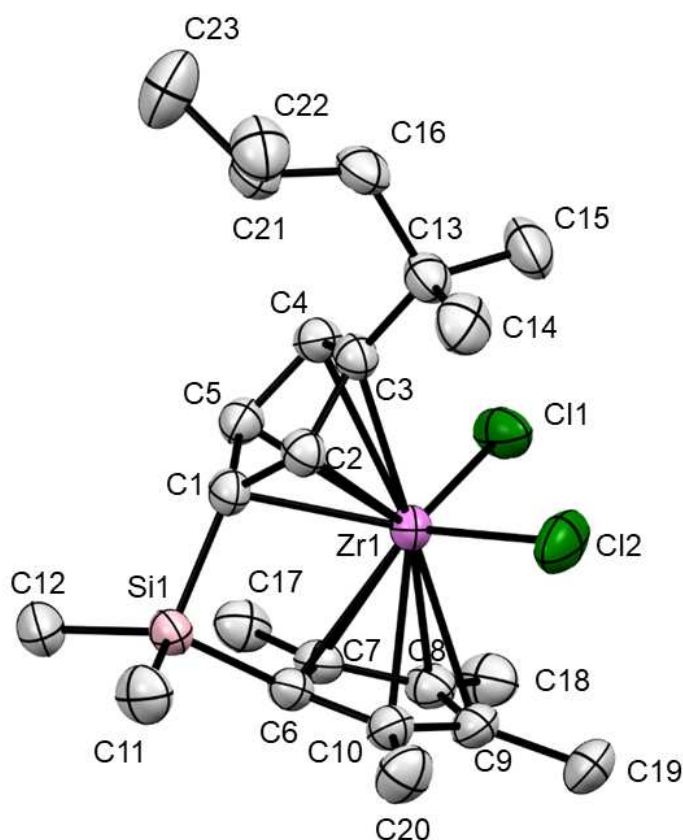


Figure 4. Molecular structure and atom-labelling scheme for $[\text{Zr}\{\text{Me}_2\text{Si}(\eta^5\text{-C}_5\text{Me}_4)(\eta^5\text{-C}_5\text{H}_3\{\text{CMe}_2\text{CH}_2\text{CHMe}_2\})\}\text{Cl}_2]$ (**9**) with ellipsoids at 30% probability (hydrogen atoms are omitted for clarity)

The η^5 coordination mode of the cyclopentadienyl rings of the zirconium atom and a distorted tetrahedral environment (bond angle Cent1–Zr1–Cent2 cent1 of $127.3(2)^\circ$) were confirmed by this study. This bond angle, although similar to those found in other *ansa*-metallocene complexes [8], is slightly lower than that found for compound **6** directly due to the presence of the *ansa*-bridge.

The angles involving the carbon atoms of the alkyl chain are close to 109.5° again indicating the sp^3 hybridization of these atoms. This fact is confirmed considering the bond distances values between these carbon atoms that are close to 1.54 \AA (C–C single bond).

Finally, and with respect to the *ansa*-bridge, the distance between the silicon atom and each of the four carbon atoms, are close to the value of 1.86 \AA , in addition, the C1–Si1–C6 and C11–Si1–C12 angles are of $94.9(1)$ and $108.3(2)$, respectively, slightly distorted from the tetrahedral geometry of the silicon atom. Furthermore, the angles Si1–C1–Cent1 and Si1–C6–Cent2 are of $163.0(2)$ and $162.0(2)$, respectively, and show the slight distortion of the planarity of the cyclopentadienyl rings.

Table 3. Selected Bond Lengths (\AA) and Angles ($^\circ$) for **9**^a

Bond Lengths (\AA)	9
Zr1–Cent1	2.235(2)
Zr1–Cent2	2.224(2)
Zr1–Cl1	2.4291(8)
Zr1–Cl2	2.4168(8)
Si1–C1	1.872(3)
Si1–C6	1.885(3)
Si1–C11	1.849(3)
Si1–C12	1.857(3)
C1–C2	1.419(4)
C3–C4	1.405(4)
C6–C7	1.437(4)
C8–C9	1.400(4)
C13–C14	1.520(5)
C16–C21	1.524(5)
Angles ($^\circ$)	9
Cent1–Zr1–Cent2	127.3(2)
Cl1–Zr1–Cl2	98.77(4)
C1–Si1–C6	94.9(1)
C11–Si1–C12	108.3(2)
Si1–C1–Cent1	163.0(2)
Si1–C6–Cent2	162.0(2)
C1–C2–C3	109.9(2)
C3–C4–C5	109.0(2)
C7–C8–C9	108.6(2)
C8–C9–C10	107.8(2)
C14–C13–C15	109.6(3)
C13–C16–C21	118.5(3)
C22–C21–C23	101.7(9)

Cent1 and Cent2 refer to the centroids of C1–C5 and C6–C10, respectively.

3.6. Ethylene polymerization studies

Ethylene polymerization studies have been carried out using the metallocene complexes **1**, **2**, **5**, **6** and **9** as catalysts. The parent titanocene and zirconocene derivatives $[\text{M}(\eta^5\text{-C}_5\text{H}_5)_2\text{Cl}_2]$ (M = Ti, Zr) have been tested as reference catalysts.

The polymerization experiments were carried out using $7.5 \text{ }\mu\text{moles}$ of catalyst and methylaluminoxane (MAO) in a Al:Ti 1000:1 ratio. The time and temperature of all experiments were 60 minutes and at temperatures of 10 , 40 and $80 \text{ }^\circ\text{C}$, respectively, using 2.0 bar of

monomer pressure. The catalytic activities (in kg PE/mol_M·h), as well as the polymer molecular weight and distribution values (polydispersity) are given in Table 4.

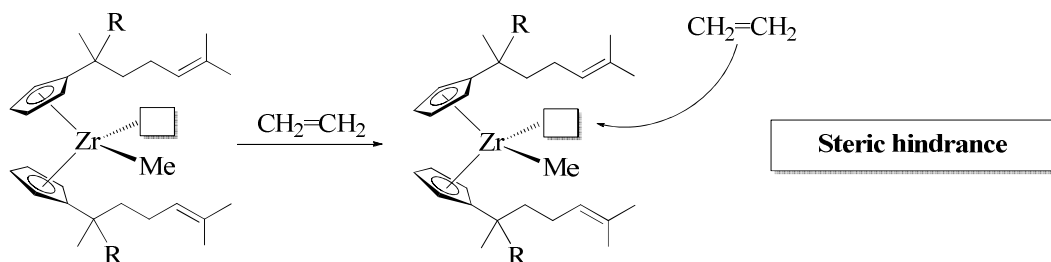
Table 4. Ethylene polymerization results for **1**, **2**, **5**, **6**, and **9** and [M(η⁵-C₅H₅)₂Cl₂] (M = Ti, Zr) ^a

Catalysts	Temperature (°C)	Activity ^b	M _w	M _w /M _n
[Ti(η ⁵ -C ₅ H ₅) ₂ Cl ₂]	10	Inactive	-	-
	40	315	51000	3.2
	80	Inactive	-	-
[Ti(η ⁵ -C ₅ H ₄ {CMe ₂ CH ₂ CHMe ₂ }) ₂ Cl ₂] (5)	10	Inactive	-	-
	40	Inactive	-	-
	80	Inactive	-	-
[Zr(η ⁵ -C ₅ H ₅) ₂ Cl ₂]	10	1830	859336	3.61
	40	3704	436969	3.65
	80	12716	73182	2.92
[Zr(η ⁵ -C ₅ H ₄ {CMe ₂ CH ₂ CH ₂ CH=CM ₂ }) ₂ Cl ₂] (1)	10	981	848370	3.10
	40	1409	450825	4.43
	80	661	119962	5.47
[Zr(η ⁵ -C ₅ H ₄ {CMePhCH ₂ CH ₂ CH=CM ₂ }) ₂ Cl ₂] (2)	10	Inactive	-	-
	40	Inactive	-	-
	80	Inactive	-	-
[Zr(η ⁵ -C ₅ H ₄ {CMe ₂ CH ₂ CHMe ₂ }) ₂ Cl ₂] (6)	10	980	818515	4.88
	40	1001	545169	4.76
	80	841	234637	5.65
[Zr{Me ₂ Si(η ⁵ -C ₅ Me ₄)(η ⁵ -C ₅ H ₃ {CMe ₂ CH ₂ CHMe ₂ })}Cl ₂] (9)	10	56	345286	4.16
	40	311	221645	2.52
	80	345	147508	3.61

^a 2 bar monomer pressure, 200 mL toluene, t_{pol} = 60 min.

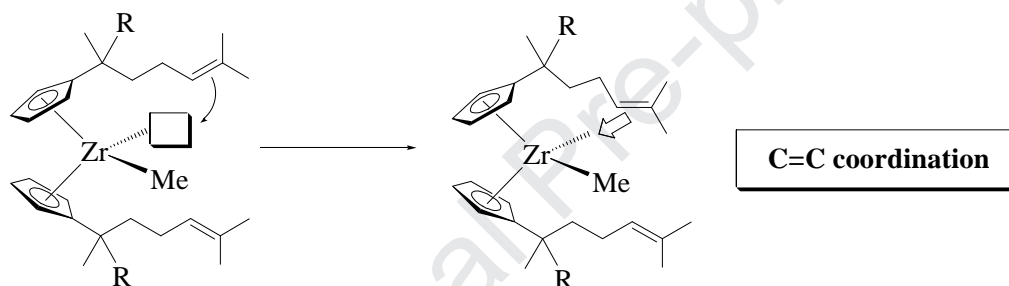
^b In kg polymer / (mol_M h bar).

In general, at all the studied temperatures, the zirconocene complexes were less active than the reference catalyst [Zr(η⁵-C₅H₅)₂Cl₂], indicating that the introduction of alkenyl or bulky alkyl substituents on the cyclopentadienyl rings leads to a significant decrease in the catalytic activity of these compounds. This fact can be explained principally based on steric hindrance (Scheme 4) which may impede olefin coordination in the catalytic cycle and decrease of catalytic activity in ethylene polymerization.



Scheme 4. Steric hindrance consideration in ethylene polymerization

For the alkenyl complexes **1** and **2** an additional factor is the possible intramolecular interaction of the ligand with the zirconium metal centre that would block the vacant site and prevent olefin coordination (Scheme 5). This phenomenon has been previously observed [33,34]. In fact, complex **2** proved to be non-responsive as a catalyst under the tested experimental conditions.



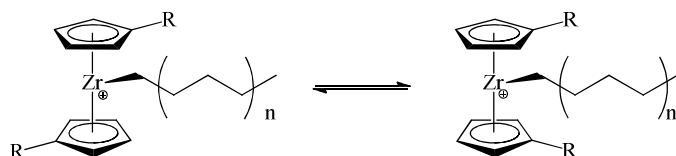
Scheme 5. C=C intramolecular coordination to the metal centre.

The titanocene complex **5**, showed no catalytic activity at any of the studied temperatures under the mild experimental conditions used in the polymerization. In addition, the reference complex $[\text{Ti}(\eta^5\text{-C}_5\text{H}_5)_2\text{Cl}_2]$ only presented catalytic activity at 40 °C, which confirms that the well-known fact that titanium-based metallocene complexes are far less active than their zirconium counterparts.

In general increasing temperature gives higher catalytic activities. However, for **1** and **6**, activities at 80 °C were lower to those recorded at 40 and 10 °C. Variation in temperature for **1**, **6** and **9** is not nearly as influential as that experienced by the reference catalyst $[\text{Zr}(\eta^5\text{-C}_5\text{H}_5)_2\text{Cl}_2]$ (see Table 5). The highest catalytic activity was observed for **6** at 40 °C (1409 kg PE/mol_{Zr}·h bar).

Polyethylene molecular weights obtained with the catalyst **1**, **6** and **9** were between 119000 and 850000 g/mol, being similar to the molecular weights of the polymers obtained with the reference catalyst at each temperature. Molecular weights decreased on increasing the polymerization temperature.

Polydispersity values of the polymers obtained are close to 3, being slightly higher than those for polymers obtained with single-site catalysts. This slight broadening of the molecular weight distribution (polydispersity) is probably due to the chemical equilibrium between the two possible rotamers of metallocene complexes, generating the existence of several active sites (Scheme 6).



Scheme 6. Rotamers in the case of disubstituted zirconocene complex.

The best value of polydispersity ($M_w/M_n = 2.52$) was recorded for the polyethylene produced with the *ansa*-metallocene complex **9** at 40 °C. The *ansa*-bridge impedes the rotation of the cyclopentadienyl ring making a more fixed environment around the zirconium metal centre.

4. Conclusions

New alkenyl and alkyl substituted group 4 metallocene(IV). dichloride complexes have been synthesized and characterized. The molecular structures of **5**, **6** and **9** have been determined and reveal the typical bent metallocene conformation. The metallocene complexes were tested as catalysts in the polymerization of ethylene with only the zirconocene complexes **1**, **6** and **9** showing catalytic activity. The alkenyl and alkyl substituents were shown to negatively influence the catalytic activity probably due to steric hindrance and in the case of the alkenyl substituted zirconocene **1** and **2** by intermolecular coordination blocking the vacant site from ethylene monomer coordination.

Acknowledgements

We gratefully acknowledge financial support from the Ministerio de Ciencia, Innovación y Universidades of Spain (Grant no. RTI2018-094322-B-I00).

Appendix A. Supplementary material

CCDC 1915969-1915971 contain the supplementary crystallographic data for this paper. These data can be obtained free of charge from the Cambridge Crystallographic Data Centre via www.ccdc.cam.ac.uk/data_request/cif.

Supplementary data to this article can be found online at ...

References

- [1] N.J. Long, *Metallocenes: An Introduction to Sandwich Complexes*, Wiley, 1998.

- [2] A. Togni, R.L. Halterman, *Metallocenes: synthesis, reactivity, applications*, Wiley-VCH, 1998.
- [3] M.M. Santos, P. Bastos, I. Catela, K. Zalewska, L.C. Branco, Recent Advances of Metallocenes for Medicinal Chemistry, *Mini Rev Med Chem.* 17 (2017) 771–784. doi:10.2174/1389557516666161031141620.
- [4] T. Takahashi, ed., *Metallocenes in Regio- and Stereoselective Synthesis*, Springer-Verlag, Berlin Heidelberg, 2005. <https://www.springer.com/la/book/9783540016069> (accessed May 14, 2019).
- [5] J.B.P. Soares, A.E. Hamielec, Metallocene/Aluminoxane Catalysts for Olefin Polymerization. A Review, *Polymer Reaction Engineering.* 3 (1995) 131–200. doi:10.1080/10543414.1995.11671695.
- [6] H.G. Alt, A. Köppl, Effect of the Nature of Metallocene Complexes of Group IV Metals on Their Performance in Catalytic Ethylene and Propylene Polymerization, *Chem. Rev.* 100 (2000) 1205–1222. doi:10.1021/cr9804700.
- [7] G.W. Coates, Precise Control of Polyolefin Stereochemistry Using Single-Site Metal Catalysts, *Chem. Rev.* 100 (2000) 1223–1252. doi:10.1021/cr990286u.
- [8] S. Prashar, A. Antiñolo, A. Otero, Insights into group 4 and 5 ansa-bis(cyclopentadienyl) complexes with a single-atom bridge, *Coordination Chemistry Reviews.* 250 (2006) 133–154. doi:10.1016/j.ccr.2005.05.017.
- [9] A. Antiñolo, M. Fajardo, S. Gómez-Ruiz, I. López-Solera, A. Otero, S. Prashar, A.M. Rodríguez, Group 4 metallocene complexes incorporating vinyl or allyl substituted ansa ligands. X-Ray crystal structures of $[\text{Zr}\{\text{Me}(\text{CH}_2=\text{CH})\text{Si}(\eta^5\text{-C}_5\text{Me}_4)_2\}\text{Cl}_2]$, $[\text{Zr}\{\text{Me}(\text{CH}_2=\text{CHCH}_2)\text{Si}(\eta^5\text{-C}_5\text{H}_4)_2\}\text{Cl}_2]$ and $[\text{Zr}\{\text{Me}(\text{CH}_2=\text{CHCH}_2)\text{Si}(\eta^5\text{-C}_5\text{Me}_4)(\eta^5\text{-C}_5\text{H}_4)\}\text{Cl}_2]$, *Journal of Organometallic Chemistry.* 683 (2003) 11–22. doi:10.1016/S0022-328X(03)00166-9.
- [10] A. Antiñolo, M. Fajardo, S. Gómez-Ruiz, I. López-Solera, A. Otero, S. Prashar, Hydrosilylation in the Design and Functionalization of ansa-Metallocene Complexes, *Organometallics.* 23 (2004) 4062–4069. doi:10.1021/om049791u.
- [11] S. Gómez-Ruiz, S. Prashar, M. Fajardo, A. Antiñolo, A. Otero, M.A. Maestro, V. Volkis, M.S. Eisen, C.J. Pastor, Synthesis, hydrosilylation reactivity and catalytic properties of group 4 ansa-metallocene complexes, *Polyhedron.* 24 (2005) 1298–1313. doi:10.1016/j.poly.2005.03.056.
- [12] S. Gómez-Ruiz, S. Prashar, L.F. Sánchez-Barba, D. Polo-Cerón, M. Fajardo, A. Antiñolo, A. Otero, M.A. Maestro, C.J. Pastor, Synthesis and catalytic applications of C1 symmetric group 4 ansa-metallocene complexes, *Journal of Molecular Catalysis A: Chemical.* 264 (2007) 260–269. doi:10.1016/j.molcata.2006.09.011.
- [13] D. Polo-Cerón, S. Gómez-Ruiz, S. Prashar, M. Fajardo, A. Antiñolo, A. Otero, I. López-Solera, M.L. Reyes, Synthesis of chiral unbridged zirconocene complexes: Applications in the polymerization of ethylene and propylene, *Journal of Molecular Catalysis A: Chemical.* 268 (2007) 264–276. doi:10.1016/j.molcata.2006.12.040.
- [14] D. Polo-Cerón, S. Gómez-Ruiz, J. Ceballos-Torres, S. Prashar, M. Fajardo, M.L. Reyes, Synthesis and structural characterization of novel three carbon atom bridged ansa-bis(indenyl)zirconocene complexes: Applications in ethylene polymerization, *Polyhedron.* 80 (2014) 129–133. doi:10.1016/j.poly.2014.02.033.
- [15] U. Romano, F. Garbassi, The environmental issue. A challenge for new generation polyolefins, *Pure and Applied Chemistry.* 72 (2000) 1383–1388. doi:10.1351/pac200072071383.
- [16] D.W. Sauter, M. Taoufik, C. Boisson, Polyolefins, a Success Story, *Polymers.* 9 (2017) 185. doi:10.3390/polym9060185.
- [17] The future of plastic, *Nature Communications.* 9 (2018) 2157. doi:10.1038/s41467-018-04565-2.
- [18] M.R. Machat, A. Fischer, D. Schmitz, M. Vöst, M. Drees, C. Jandl, A. Pöthig, N.P.M. Casati, W. Scherer, B. Rieger, Behind the Scenes of Group 4 Metallocene Catalysis: Examination of the Metal–Carbon Bond, *Organometallics.* 37 (2018) 2690–2705. doi:10.1021/acs.organomet.8b00339.
- [19] M.E.Z. Velthoen, A. Muñoz-Murillo, A. Bouhmadi, M. Cecius, S. Diefenbach, B.M. Weckhuysen, The Multifaceted Role of Methylaluminoxane in Metallocene-Based Olefin Polymerization Catalysis, *Macromolecules.* 51 (2018) 343–355. doi:10.1021/acs.macromol.7b02169.

- [20] X. Wang, X. Han, F. Ren, R. Xu, Y. Bai, Porous Organic Polymers-Supported Metallocene Catalysts for Ethylene/1-Hexene Copolymerization, *Catalysts*. 8 (2018) 146. doi:10.3390/catal8040146.
- [21] S. Gómez-Ruiz, D. Polo-Cerón, S. Prashar, M. Fajardo, A. Antiñolo, A. Otero, Synthesis and Reactivity of Alkenyl-Substituted Zirconocene Complexes and Their Application as Olefin Polymerisation Catalysts, *European Journal of Inorganic Chemistry*. 2007 (2007) 4445–4455. doi:10.1002/ejic.200700394.
- [22] S. Gómez-Ruiz, D. Polo-Cerón, S. Prashar, M. Fajardo, V.L. Cruz, J. Ramos, E. Hey-Hawkins, Synthesis, characterization and catalytic behaviour of ansa-zirconocene complexes containing tetraphenylcyclopentadienyl rings: X-ray crystal structures of $[\text{Zr}\{\text{Me}_2\text{Si}(\eta^5\text{-C}_5\text{Ph}_4)(\eta^5\text{-C}_5\text{H}_3\text{R})\}\text{Cl}_2]$ ($\text{R}=\text{H}$, But), *Journal of Organometallic Chemistry*. 693 (2008) 601–610. doi:10.1016/j.jorganchem.2007.11.054.
- [23] S. Gómez-Ruiz, G.N. Kaluđerović, D. Polo-Cerón, V. Tayurskaya, S. Prashar, M. Fajardo, R. Paschke, A novel alkenyl-substituted ansa-zirconocene complex with dual application as olefin polymerization catalyst and anticancer drug, *Journal of Organometallic Chemistry*. 694 (2009) 3032–3038. doi:10.1016/j.jorganchem.2009.05.013.
- [24] J. Ceballos-Torres, P. Virag, M. Cenariu, S. Prashar, M. Fajardo, E. Fischer-Fodor, S. Gómez-Ruiz, Anti-cancer Applications of Titanocene-Functionalised Nanostructured Systems: An Insight into Cell Death Mechanisms, *Chemistry – A European Journal*. 20 (2014) 10811–10828. doi:10.1002/chem.201400300.
- [25] A. Antiñolo, I. López-Solera, I. Orive, A. Otero, S. Prashar, A.M. Rodríguez, E. Villaseñor, Niobium and Zirconium Complexes Incorporating Asymmetrically Substituted ansa Ligands. X-ray Crystal Structures of $[\text{Me}_2\text{Si}(\eta^5\text{-C}_5\text{Me}_4)(\eta^5\text{-C}_5\text{H}_3\text{R})]\text{Nb}(\text{N}^i\text{Bu})\text{Cl}$ ($\text{R} = \text{Me}$, ^iPr) and $[\text{Me}_2\text{Si}(\eta^5\text{-C}_5\text{Me}_4)(\eta^5\text{-C}_5\text{H}_3\text{R})]\text{ZrCl}_2$ ($\text{R} = \text{H}$, Me), *Organometallics*. 20 (2001) 71–78. doi:10.1021/om0006662.
- [26] K.J. Stone, R.D. Little, An exceptionally simple and efficient method for the preparation of a wide variety of fulvenes, *J. Org. Chem.* 49 (1984) 1849–1853. doi:10.1021/jo00185a001.
- [27] SCALE3 ABSPACK - Empirical absorption correction. CrysAlis Software Package, Oxford Diffraction Ltd., 2006.
- [28] G.M. Sheldrick, SHELXS-97; University of Göttingen: Göttingen, Germany, 1997; Sheldrick, *Acta Crystallogr., Sect. A*. 46 (1990) 467–473.
- [29] G.M. Sheldrick, SHELXL-97, Program for crystal structure refinement; University of Göttingen: Göttingen, Germany, 1997.
- [30] S. Gómez-Ruiz, G.N. Kaluđerović, D. Polo-Cerón, S. Prashar, M. Fajardo, Ž. Žižak, Z.D. Juranić, T.J. Sabo, Study of the cytotoxic activity of alkenyl-substituted ansa-titanocene complexes, *Inorganic Chemistry Communications*. 10 (2007) 748–752. doi:10.1016/j.inoche.2007.03.016.
- [31] J. Ceballos-Torres, S. Gómez-Ruiz, G.N. Kaluđerović, M. Fajardo, R. Paschke, S. Prashar, Naphthyl-substituted titanocene dichloride complexes: Synthesis, characterization and in vitro studies, *Journal of Organometallic Chemistry*. 700 (2012) 188–193. doi:10.1016/j.jorganchem.2011.12.015.
- [32] J. Ceballos-Torres, M.J. Caballero-Rodríguez, S. Prashar, R. Paschke, D. Steinborn, G.N. Kaluđerović, S. Gómez-Ruiz, Synthesis, characterization and in vitro biological studies of titanocene(IV) derivatives containing different carboxylato ligands, *Journal of Organometallic Chemistry*. 716 (2012) 201–207. doi:10.1016/j.jorganchem.2012.06.028.
- [33] A.I. Licht, H.G. Alt, Synthesis of novel metallacyclic zirconocene complexes from ω -alkenyl-functionalized zirconocene dichloride complexes and their use in the α -olefin polymerization, *Journal of Organometallic Chemistry*. 648 (2002) 134–148. doi:10.1016/S0022-328X(01)01454-1.
- [34] M. Lamač, M. Horáček, J. Kubišta, J. Pinkas, Intramolecular activation of pendant alkenyl group as a tool for modification of the zirconocene framework, *Inorganica Chimica Acta*. 373 (2011) 291–294. doi:10.1016/j.ica.2011.03.061.

Highlights

- New alkenyl and alkyl substituted group 4 metallocene complexes have been synthesized and characterized.
- Molecular structures of titanocene and zirconocene complexes have been determined.
- Metallocene complexes have been studied as catalysts in ethylene polymerization.